

Study of Mg₆Pd alloy synthesized by cold rolling

J. Dufour, J. Huot*

*Institut de Recherche sur l'Hydrogène, Université du Québec à Trois-Rivières,
3351, Boul. Des Forges, Trois-Rivières, Que. G9A 5H7, Canada*

Received 26 October 2006; received in revised form 28 November 2006; accepted 29 November 2006
Available online 2 January 2007

Abstract

In this paper we report the hydrogen storage properties of Mg₆Pd alloy synthesized by cold rolling and ball milling followed by heat treatment. The heat treatment was performed at 623 K, a much lower temperature than the peritectic temperature of Mg₆Pd (973 K). After heat treatment the reaction is complete. The laminated sample is much easier to activate under hydrogen and has a better resistance to air exposure than the ball-milled sample. The hydrogenation is a reversible disproportionation reaction with generation of magnesium hydride and Mg₅Pd₂ alloy. The hydrogenation pressure–composition curve shows the presence of two plateaus: the first plateau corresponds to the decomposition of Mg₆Pd into Mg_{78.5}Pd_{21.5} and MgH₂ while the second plateau is the decomposition of Mg_{78.5}Pd_{21.5} into Mg₅Pd₂ and MgH₂. As the only hydride phase is MgH₂, the dehydrogenation curves show only the plateau corresponding to magnesium hydride. Cold rolling is proved to be an efficient and easy way to synthesize Mg–Pd intermetallics.

© 2006 Elsevier B.V. All rights reserved.

Keywords: Hydrogen storage materials; Magnesium; Palladium; Activation; Cold rolling; Intermetallics

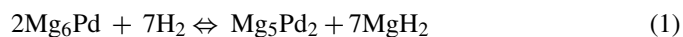
1. Introduction

Metal hydrides are considered valuable candidates as hydrogen storage material for future clean energy systems. However, to reach commercial application many problems such as hydrogen storage capacity, resistance to impurities, stability under cycling, and sorption kinetics have to be solved. Cost of raw materials and processing should also be reduced. Recently, a low cost and easily scalable technique, cold rolling, has been investigated as a mean to synthesize and modify metal hydrides alloys [1–4].

Because of their high hydrogen storage capacity, magnesium and magnesium-based alloys are actively investigated as hydrogen-storage materials. To improve the slow sorption kinetics, additions of various catalysts have been investigated. Palladium, while being too expensive to be really integrated in a future application for hydrogen storage, greatly improves hydrogen storage properties of magnesium [5–9] and air resistance [10,11]. Moreover, Mg–Pd thin films have interesting optical properties [7,12,13]. Consequently, study of Mg–Pd sys-

tem could give valuable insight for the synthesis of other more practical systems.

In a previous work on Mg–Pd 2.5 at% system we have shown that after cold rolling and mild heat treatment there is formation of the intermetallic compound Mg₆Pd [4]. This alloy has the lowest peritectic point in the Mg–Pd phase diagram [14] and is considered to be the most interesting for hydrogen storage [15]. The hydrogen storage properties of Mg₆Pd have been investigated by Kume and Weiss [15] and Yamada et al. [16]. In these two studies, the intermetallic alloy was produced by mixing the raw elements and melting at temperature above 1070 K. Upon hydrogenation, Mg₆Pd was believed to decompose into Mg₅Pd₂ alloy and magnesium hydride in a reversible disproportionation reaction:



With respect to the Mg₆Pd molecular weight, this reaction takes 2.8 wt% of hydrogen. According to Kume and Weiss, hydrogen reaction with Mg₆Pd is mainly driven by the reaction of hydrogen with the magnesium atoms, palladium being of minor interest [15]. They explained this behavior by the combination of the ionic and covalent character of the Mg–H bond [17]. Yamada et al. observed a second plateau in their

* Corresponding author. Fax: +1 819 376 5164.
E-mail address: jacques.huot@uqtr.ca (J. Huot).

dehydrogenation curves of $\text{Mg}_{89}\text{Pd}_{11}$, which they explain as possibly the formation of a $\text{Mg}_5\text{Pd}_2\text{H}_{\sim 5}$ hydride [16].

In this study, we investigated the synthesis of Mg_6Pd alloy by cold rolling and ball milling of raw elements. For both techniques a mild heat treatment was necessary to obtain complete alloy formation. The hydrogen sorption kinetics and pressure–composition curves were investigated, with a special emphasis on the reaction mechanism and decomposition steps.

2. Experimental method

Cold-rolled samples were prepared using a manual rolling apparatus with 75 mm diameter roll. Pure magnesium from a Norsk Hydro ingot were cut into small square pieces (5 mm thick, 1 cm side), then rolled a single time to a thickness of 1 mm. Palladium foil (Aldrich, 0.025 mm thick, 99.99%) was used as starting material. The metals were stacked in a (mg–pd–mg–pd–mg) configuration, while keeping the correct stoichiometry of Mg (86 at%), Pd (14 at%). The stack was inserted between two stainless steel (316) protective sheets, and then rolled 20 times in air, folding the sample between each roll. Thus, a layer reduction of 50% was performed at each rolling. After 20 rollings, the samples were a homogenous looking metal of 0.40 mm thickness. The rolled samples were stored in air prior to hydrogen activation and sorption measurements.

The same starting elements were used to synthesize the ball-milled sample of identical stoichiometry as cold rolled. To prevent sticking of magnesium in the crucible, magnesium pieces were cold-rolled thirty times before ball milling. The magnesium and palladium were cut into small pieces, and then put in a 55 cm³ crucible, with three stainless steel balls for a powder to balls weight ratio of 30. A high-energy shaker mill (Spex 8000) was used. After 10 h of milling in argon atmosphere, a fine powder was collected and stored under argon.

The hydrogen sorption properties of the samples were measured with a Sievert-type apparatus. Before activation, the sample was heated to a temperature of 623 K while being kept under a 0.01 MPa vacuum. To activate the samples, they were exposed to a hydrogen pressure of 1.33 MPa under a constant temperature of 623 K. Kinetics measurements were done at 623 K under 1.33 MPa of pressure for hydrogenation and 0.01 MPa for dehydrogenation. Crystal structure was investigated by X-ray diffraction using a Rigaku D-max diffractometer using Cu K α radiation. The same set of scattered slits was used for all powder diffraction patterns. However, the background at lower angles is in general more visible in the case of cold-rolled samples due to the smaller signal/noise ratio.

3. Results

3.1. As prepared cold-rolled and ball-milled samples

Fig. 1 shows the X-ray patterns of the ball-milled and cold-rolled samples. The pattern of as-rolled sample shows a preferred orientation of the (002) peak as expected for a laminated material. Even though both samples have the same stoichiometry, the palladium peaks are clearly shown on the as-rolled pattern but are practically absent in the as-milled pattern. A similar effect was seen previously and could be explained by the palladium particle size, which is an order of magnitude bigger in the case of cold-rolled sample compared to ball-milled sample [4].

3.2. Activation and kinetics of the Mg–Pd samples

Once synthesized, the samples were hydrogen activated by exposing them to a hydrogen pressure of 1.3 MPa at 623 K. The activation curves of cold-rolled and ball-milled samples are shown in Fig. 2. The striking difference is that the cold-rolled

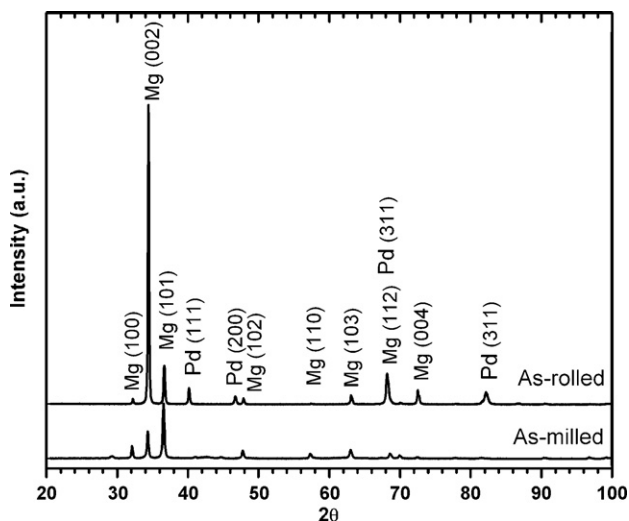


Fig. 1. X-ray powder diffraction patterns of 6Mg + Pd samples prepared by cold rolling and ball milling. Small peaks at 29, 41, and 46° belong to magnesium oxide phase.

sample does not present an incubation time contrary to the ball-milled sample, which presents an incubation time of about 400 min. Moreover, the activation kinetics is very fast from the beginning and the full capacity is reached in 2000 min. Full capacity is not reached for the ball-milled sample even after 4000 min. A few hydrogen hydrogenation/dehydrogenation cycles had to be performed before reaching full capacity.

It may be argued that the relatively poor vacuum (0.01 MPa) caused some oxidation before activation. It should be pointed out that this vacuum was also reached before kinetic measurements. If some in situ oxidation was present, it would also have been seen in the kinetic measurements, which was not the case.

After both samples were fully activated, kinetics measurements were performed. Results are shown in Fig. 3. The hydrogenation kinetic of the cold-rolled sample is very similar to its activation curve. Both curves have the same shape and a hydrogen capacity of 2.0 wt% is reached after 200 min in both cases. Thus, for cold-rolled sample the activation process

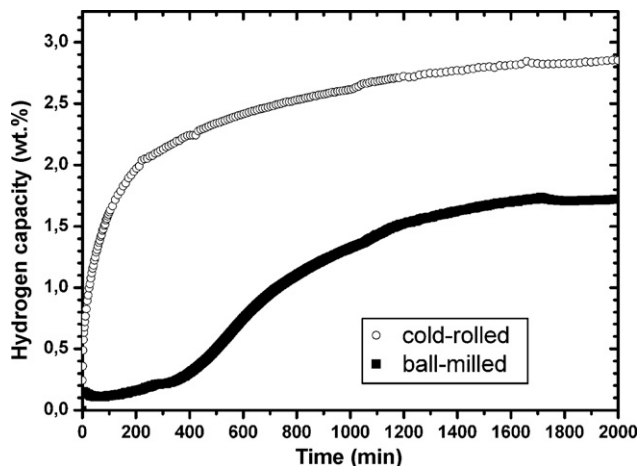


Fig. 2. Activation curve of cold-rolled and ball-milled 6Mg + Pd samples. Activation temperature 623 K, pressure 1.3 MPa.

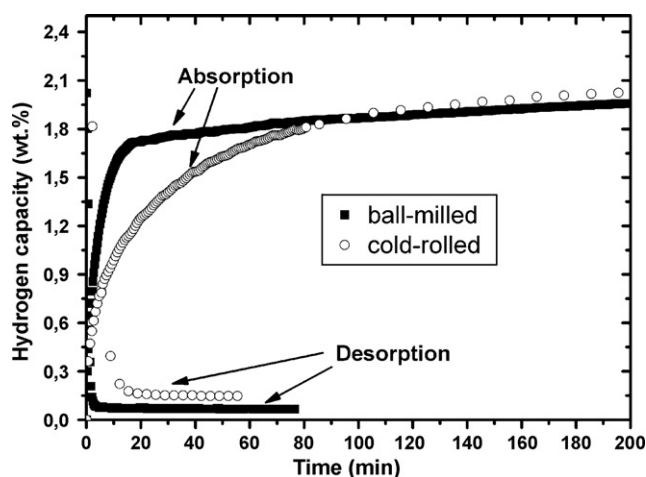


Fig. 3. Hydrogen sorption kinetics at 623 K of cold-rolled and ball-milled 6Mg + Pd samples. Hydrogenation pressure 1.0 MPa, dehydrogenation pressure 0.06 MPa.

is essentially unnecessary. On the other hand, the hydrogenation of the ball-milled sample was greatly improved after activation. In fact, up to hydrogen capacity of 1.8 wt%, the hydrogenation is faster than for the cold-rolled sample. However, from 1.8 wt% to full capacity the reaction is very slow. On the contrary, the cold-rolled sample shows a continuous curve from the dehydrided state up to full hydrogen capacity.

The dehydrogenation kinetics curves are continuous for both cold-rolled and ball-milled samples. The ball-milled dehydrogenation kinetics is ten times faster than the cold-rolled one, taking only 2 min while the dehydrogenation of the cold-rolled sample ends in 20 min.

3.3. Rates limiting steps

Determination of the rates limiting steps of the reactions could give insight on the hydrogen sorption mechanism. Rate limiting steps were calculated following the procedure of Barkhordarian et al. [18]. Dehydrogenation for both samples is controlled by contracting volume, three-dimensional growths with constant interface velocity. Reaction constants (k) for ball-milled and cold-rolled samples are respectively -1.05×10^{-2} and -1.05×10^{-3} . In this type of reaction it is assumed that initial nucleation is fast compared to the overall growth kinetics. The constant interface velocity means that hydrogen diffusion is not rate limiting.

As seen in Fig. 3, hydrogenation kinetic of ball-milled sample is formed by two parts: the first part (up to 1.8 wt%) is regulated by contracting volume, three-dimensional growth with decreasing interface velocity ($k = 1.5 \times 10^{-4}$). Here, the decreasing velocity arises because diffusion through the transformed phase (in the present case magnesium hydride) is the rate-limiting step. The second part of hydrogenation curve of ball-milled sample (from 1.8 wt% up to full capacity) is controlled by contracting volume, two-dimensional growth with constant interface velocity ($k = 3.5 \times 10^{-5}$). This means that the hydrogen diffusion is relatively fast and the rate-limiting step is the constant velocity of the metal/hydride interface.

In the case of the cold-rolled sample, the hydrogenation kinetics is controlled by contracting volume, three-dimensional growth with decreasing surface velocity ($k = 3.52 \times 10^{-6}$). This is the same type as the first hydrogenation step of the ball-milled sample.

3.4. Pressure–composition isotherms

Fig. 4 presents the pressure–composition isotherms of cold-rolled and ball-milled samples. For the ball-milled sample the hydrogenation curve shows two distinct plateaus. The maximum hydrogen capacity of the first plateau is 1.8 wt%, which is exactly the capacity reached through the fast reaction (three-dimensional, decreasing surface velocity) shown in the kinetic curve. The second plateau therefore corresponds to the two-dimensional growth reaction with constant interface velocity.

In the case of cold-rolled sample the hydrogenation curve does not show a sharp step between the two plateaus. Instead, the first plateau is sloped, probably due to the stress induced by rolling. The second plateau is at slightly higher pressure than in the ball-milled case. Again, this may be due to induced stress in the material. The fact that the transition between the two plateaus is less steep in the cold-rolled sample than in the ball-milled one is in agreement with the hydrogenation kinetics shown in Fig. 3 where a smooth curve with a single rate limiting step identical to the first plateau of the ball-milled sample (three-dimensional, decreasing surface velocity) but with a much smaller rate constant.

Dehydrogenation isotherm of both cold-rolled and ball-milled samples shows a single plateau which pressure corresponds to dehydrogenation of magnesium hydride. This thus confirms the recombination reaction of magnesium and Mg_5Pd_2 to form Mg_6Pd .

3.5. X-ray powder diffraction

The crystal structures in fully hydrided state were investigated by first hydriding a sample at high temperature (623 K)

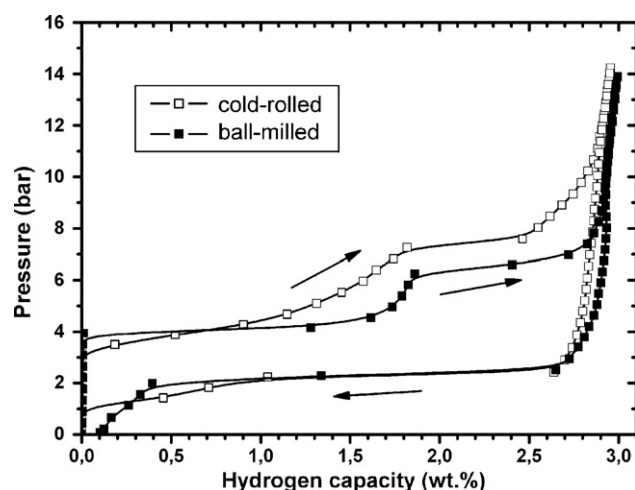


Fig. 4. Pressure–composition isotherms at 623 K of cold-rolled and ball-milled 6Mg + Pd samples.

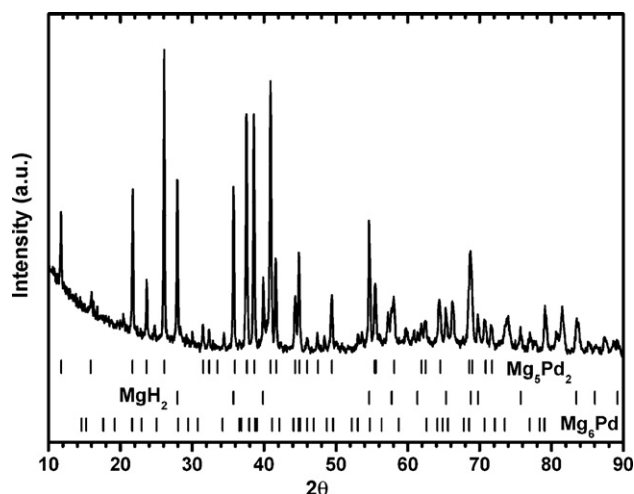


Fig. 5. X-ray powder diffraction patterns of cold-rolled 6Mg + Pd sample in the hydrogenated state.

and quenching it at room temperature while being kept under high hydrogen pressure. Fig. 5 shows the X-ray pattern of cold-rolled sample in a fully hydrided state. As stated in Eq. (1) the hydrided state is formed by magnesium hydride and Mg_5Pd_2 alloy. No peaks belonging to Mg_6Pd are found. The powder diffraction patterns of dehydrided cold-rolled and ball-milled samples are shown in Fig. 6. For both samples, only Mg_6Pd phase is seen, thus proving the reversibility of reaction (1).

4. Discussion

The first notable effect found in this study was the fast hydrogen activation of the cold-rolled sample. In fact, the sample absorbs hydrogen as fast in the first cycle as in the subsequent cycles. In comparison, the activation of the ball-milled sample is slow and presents a long incubation time. The superior behavior of cold-rolled sample is even more remarkable considering the fact that the ball milling was performed under inert atmosphere and the powder was stored under argon before measurement

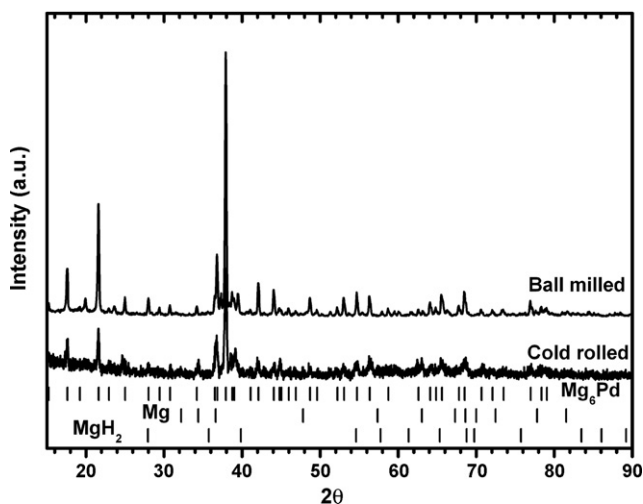


Fig. 6. X-ray powder diffraction patterns of cold-rolled and ball-milled 6Mg + Pd samples after hydrogen cycling.

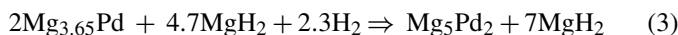
while cold rolling was performed in air and the rolled sample kept in air without any protection.

The second noteworthy effect is the presence of a second plateau in the hydrogenation pressure–composition isotherm. In their work, Yamada et al. [16] identified the lower plateau of the dehydrogenation curve to $MgH_2 \Rightarrow Mg$ dehydrogenation, while the upper one was correlated to the reaction $Mg_6Pd \Leftrightarrow Mg_5Pd_2$. In our experiments, the fully hydrided compound is made of Mg_5Pd_2 and MgH_2 only as shown in Fig. 5. This is confirmed by the single desorbing plateau, which pressure corresponds to the dehydrogenation of magnesium hydride.

For the hydrogenation curve, the situation is more complex. It is proved by X-ray diffraction that the fully dehydrogenated state is pure Mg_6Pd . However, a direct formation of MgH_2 and Mg_5Pd_2 (reaction (1)) should not give two plateaus. Recently, a new determination of the Mg–Pd phase diagram by Makongo et al. showed the existence of intermediate phases between Mg_6Pd and Mg_5Pd_2 [19]. Complex metallic alloys of composition $Mg_{57}Pd_{13}$, $Mg_{56.4}Pd_{13.5}$, $Mg_{306}Pd_{77}$, $Mg_{78.5}Pd_{21.5}$, and Mg_3Pd were identified. We considered possible reactions with all of these alloys and we found that the reaction involving the alloy $Mg_{78.5}Pd_{21.5}$ (thereafter written $Mg_{3.65}Pd$ for better comparison with Mg_6Pd) nominally absorbs 1.86 wt% of hydrogen:



This amount of hydrogen corresponds to the first plateau of our PCT curve of the ball-milled sample. The second plateau is then the reaction:



which absorbs a further 0.91 wt% of hydrogen. Reactions (2) and (3) agree quite closely to the PCT curves of Fig. 4. It is interesting to note that the three compounds involved in reactions (2) and (3) presents homogeneity range, contrary to $Mg_{57}Pd_{13}$, $Mg_{306}Pd_{77}$, and Mg_3Pd (for $Mg_{56.4}Pd_{13.5}$ the phase boundaries are unavailable at low temperature). This may be the reason why these particular compositions react with hydrogen. In a future experiment we are planning to perform absorption to much higher pressure in order to test if the next homogeneity range ($MgPd$) is formed in reaction (4):



As Makongo et al. indicated, Mackay clusters play an important role in the phase formation of these alloys [19]. It may be interesting to investigate further the relationship of this type of clusters with hydrogen.

5. Conclusion

With this work, we showed that cold rolling is an easy and powerful method to synthesize hydrogen storage alloys. The cold-rolled alloy shows enhanced activation properties and remarkable resistance to air exposure. The pressure composition isotherm of ball-milled sample presents two distinct plateaus while for the cold-rolled sample there is a smooth transition from the lower to upper plateau. This is reflected in the hydrogenation

kinetics where the hydrogenation curve of the cold-rolled sample is driven by a single mechanism (three-dimensional, decreasing surface velocity) whereas the ball-milled sample shows different rate limiting steps for the two plateaus. From Mg–Pd phase diagram, we propose a two-step hydrogenation process, involving first the decomposition of Mg₆Pd into Mg_{78.5}Pd_{21.5} with formation of MgH₂ and a further decomposition of Mg_{78.5}Pd_{21.5} into Mg₅Pd₂ again with formation of MgH₂. The recombination is a one step reaction, going directly from Mg₅Pd₂ and MgH₂ to Mg₆Pd. Additional work is needed to confirm the reactions involved in hydrogenation and to understand the reaction mechanism, especially the relationship with Mackay clusters.

Acknowledgement

The authors wish to thank Dr. R. Bormann for helpful discussion.

References

- [1] T.T. Ueda, M. Tsukahara, Y. Kamiya, S. Kikuchi, *J. Alloys Compd.* 386 (2004) 253.
- [2] L.T. Zhang, K. Ito, V.K. Vasudevan, M. Yamaguchi, *Acta Mater.* 49 (2001) 751.
- [3] L.T. Zhang, K. Ito, V.K. Vasudevan, M. Yamaguchi, *Mater. Sci. Eng. A* 329–331 (2002) 362.
- [4] J. Dufour, J. Huot, *J. Alloys Compd.* 439 (2007) L5.
- [5] K. Higuchi, H. Kajioka, K. Toiyama, H. Fujii, S. Orimo, Y. Kikuchi, *J. Alloys Compd.* 293–295 (1999) 484.
- [6] K. Higuchi, K. Yamamoto, H. Kajioka, K. Toiyama, M. Honda, S. Orimo, H. Fujii, *J. Alloys Compd.* 330–332 (2002) 526.
- [7] H. Fujii, K. Higuchi, K. Yamamoto, H. Kajioka, S. Orimo, K. Toiyama, *Mater. Trans., JIM* 43 (11) (2002) 2721.
- [8] J. Paillier, L. Roué, *J. Alloys Compd.* 404–406 (2005) 473.
- [9] A. Léon, E.J. Knystautas, J. Huot, S. LoRusso, C.H. Koch, R. Schulz, *J. Alloys Compd.* 356–357 (2003) 530.
- [10] A. Léon, E.J. Knystautas, J. Huot, R. Schulz, *J. Alloys Compd.* 345 (2002) 158.
- [11] A. Léon, E.J. Knystautas, J. Huot, R. Schulz, *Thin Solid Films* 496 (2006) 683.
- [12] M. Pasturel, M. Slaman, H. Schreuders, J.H. Rector, D.M. Borsa, B. Dam, R. Griessen, *J. Appl. Phys.* 100 (2006) 023515.
- [13] K. Yoshimura, Y. Yamada, M. Okada, *Surf. Sci.* 566–568 (2004) 751.
- [14] B. Predel, *Landolt-Börnstein—Group IV Phys. Chem.* 5 (H) (1997) 80.
- [15] Y. Kume, A. Weiss, *J. Less Common Met.* 136 (1987) 51.
- [16] T. Yamada, J. Yin, K. Tanaka, *Mater. Trans., JIM* 42 (11) (2001) 2415.
- [17] C.M. Stander, R.A. Pacey, *J. Phys. Chem. Solids* 39 (1978) 829.
- [18] G. Barkhordarian, T. Klassen, R. Bormann, *J. Alloys Compd.* 407 (2006) 249.
- [19] J.P.A. Makongo, Yu. Prots, U. Burkhardt, R. Niewa, C. Kudla, G. Kreiner, *Philos. Mag.* 86 (3–5) (2006) 427.